Haemophilus influenzae Protein F Mediates Binding to Laminin and Human Pulmonary Epithelial Cells.

Jalalvand, Farshid; Su, Yu-Ching; Mörgelin, Matthias; Brant, Marta; Hallgren, Oskar; Westergren-Thorsson, Gunilla; Singh, Birendra; Riesbeck, Kristian

Published in:
Journal of Infectious Diseases

DOI:
10.1093/infdis/jis754

2012

Haemophilus influenzae Protein F Mediates Binding to Laminin and Human Pulmonary Epithelial Cells

Farshid Jalalvand[1], Yu-Ching Su[1], Matthias Mörgelin[2], Marta Brant[1], Oskar Hallgren[3], Gunilla Westergren-Thorsson[3], Birendra Singh[1], and Kristian Riesbeck[1]*

[1]*Medical Microbiology, Department of Laboratory Medicine Malmö, Lund University, Skåne University Hospital, Malmö, Sweden,* [2]*Section of Clinical and Experimental Infectious Medicine, Department of Clinical Sciences, Lund University, Lund, Sweden, and* [3]*Lung Biology Unit, Department of Experimental Medical Science, Lund University, Lund, Sweden*

Running title: Protein F mediates NTHi adhesion to the host

Footnote page

Potential conflicts of interest (for all authors): None.

Funding: This work was supported by grants from the Alfred Österlund, the Anna and Edwin Berger, Greta and Johan Kock, the Gyllenstiernska Krapperup, Åke Wiberg, Hans Hierta, and the Marianne and Marcus Wallenberg Foundations, the Swedish Medical Research Council (grant number 521-2010-4221, www.vr.se), the Cancer Foundation at the University Hospital in Malmö, the Physiographical Society (Forssman's Foundation), and Skåne County Council's research and development foundation.

***Correspondence:** Kristian Riesbeck, MD, Medical Microbiology, Department of Laboratory Medicine Malmö, Lund University, Skåne University Hospital, SE-205 02 Malmö, Sweden (kristian.riesbeck@med.lu.se).

ABSTRACT

The mucosal pathogen non-typeable *Haemophilus influenzae* (NTHi) adheres to the respiratory epithelium, or in the case of epithelial damage, to the underlying basement membrane and extracellular matrix that amongst other proteins consists of laminin. We have recently identified Protein F, an ABC-transporter involved in NTHi immune evasion. Homology modeling of the Protein F tertiary structure revealed a strong resemblance to the streptococcal laminin-binding proteins Lbp and Lmb. Here, we show that Protein F promotes binding of NTHi to laminin and primary bronchial epithelial cells. Analyses with recombinant proteins and synthetic peptides revealed that the N-terminal part of Protein F contains the host-interacting region. Moreover, Protein F exists in all clinical isolates, and isogenic NTHi Δ*hpf* mutants display significantly reduced binding to laminin and epithelial cells. We thus suggest Protein F to be an important and ubiquitous NTHi adhesin.

Key words: ABC-transporter, adhesion, laminin, non-typeable *Haemophilus influenzae*, Protein F, pulmonary epithelial cells, respiratory tract infection, virulence

INTRODUCTION

Non-typeable *Haemophilus influenzae* (NTHi) is a Gram-negative opportunistic pathogen that colonizes the nasopharynx of humans. It is one of the leading causes of bacterial respiratory tract infections such as acute otitis media in children and bronchitis, as well as exacerbations in patients with chronic obstructive pulmonary disease (COPD) [1-3]. To prevent clearance by the ciliated respiratory tract mucosal epithelium an important initial step of bacterial colonization is adherence to host tissue [4]. In patients suffering from disruption of the epithelial integrity caused by viral infections, mechanical damage or chronic inflammation, the underlying basement membrane is exposed to the lumen and forms a viable attachment site for pathogens [5].

The heterotrimeric glycoprotein laminin (Ln; app. 800 kDa) is one of the major constituents of the extracellular matrix (ECM) and the basement membrane. It is involved in an array of physiological functions such as cellular proliferation, migration and structural scaffolding in tissues [6-8]. During bacterial pathogenesis, Ln is frequently targeted for adherence by respiratory tract pathogens [9-16]. NTHi has previously been reported to bind Ln via the *Haemophilus* adhesion and penetration protein (Hap) and Protein E (PE) [17, 18]. In parallel, Hap and PE interact with host epithelial cells [19, 20]. These interactions are thus multifactorial, and involve several adhesins that mutually promote bacterial host-adhesion.

We recently identified a virulence factor in NTHi that we designated as Protein F (PF) (Su et al., submitted). Protein F (≈ 30 kDa) is annotated as a bacterial metal-binding receptor, belonging to the ATP-binding cassette (ABC)-transporter family. Upon

structural analysis of PF, we noticed a strong structural resemblance to the Ln-binding proteins of *Streptococcus pyogenes* (Lbp) and *S. agalactiae* (Lmb) [21, 22]. The structural similarity raised a hypothesis regarding the potential Ln-binding capacity of PF. In the present study, we show that PF is a novel surface-exposed Ln-binding protein that also promotes NTHi adherence to host epithelial cells. This is the first report that shows a direct interaction between a Gram-negative ABC-transporter protein and host components.

MATERIALS AND METHODS

Bacteria, Eukaryotic Cells, Culture Conditions, and Reagents

NTHi 3655 wild type (wt), Δ*hap* and Δ*pe* mutants, and clinical isolates KR217, KR314, KR315, KR336, KR385 obtained by nasopharyngeal swabs from patients with upper respiratory tract infection, were cultured as described [17]. Chloramphenicol (10 µg/ml) was used for selection of Δ*hpf* mutants. *Escherichia coli* BL21 (DE3) (Novagen) and DH5α (Invitrogen) were cultured in Luria-Bertani (LB) broth and solid phase medium supplemented with kanamycin (50 µg/ml) or ampicillin (100 µg/ml). The type II alveolar A549 (ATCC CCL-185) and bronchial epithelial NCI H292 (ATCC CRL-1848) cell lines were cultured in F-12 and RPMI medium (Gibco), respectively, with 10 % fetal calf serum. Primary bronchial epithelial cells were obtained from a healthy adult donor with no history of lung disease. This was approved by the Swedish Research Ethical Committee in Lund (FEK 413/2008) and written consent was obtained from the closest relatives. Cells were maintained in BEGM medium (Clonetics). All bacteria and human cells were cultured at 37°C with 5 % CO_2. Anti-PF polyclonal antibodies (pAb) were raised in rabbits and affinity purified using recombinant PF (rPF) or PF peptides [23].

Structural Modeling and Bioinformatic Analyses

Modeling of PF was performed using the Swiss-Model automated server against homologous templates available in the PDB database (www.rcsb.org). Homologs were analyzed with BLAST (http://www.ncbi.nlm.nih.gov/) and multiple alignment was performed using ClustalW (http://www.ebi.ac.uk/). Three-dimensional models were prepared using PyMOL (http://www.pymol.org/).

Construction of NTHi Δ*hpf* Mutants

Upstream (621 bp) and downstream (997 bp) flanking regions of the *hpf* gene (CGSHi3655_02309) from NTHi 3655 genomic DNA (Genbank accession number AAZF00000000) and *cat* (chloramphenicol acetyltransferase) (BAA78807) from pLysS (Novagen) were amplified (supplementary data, Table S1). Thereafter, we produced a linear knockout vector, inserting *cat* between the flanking regions, using an overlap extension PCR (supplementary Figure S1). The *hpf* gene in NTHi 3655, clinical isolates and the isogenic NTHi 3655 Δ*pe* was mutated as described [24].

Recombinant Proteins and Peptides

We amplified full length and truncated fragments of NTHi 3655 *hpf* using specific primers (Table S1). Restriction sites were introduced as indicated. pET26(b)+ (for purified recombinant proteins) or pET16b (Novagen) (for surface expression of PF) were used and transformed into *E. coli* DH5α, followed by transformation into *E. coli* BL21(DE3). Recombinant proteins were produced as described [25]. Peptides (app. 25 aa long) spanning the entire mature PF and overlapping with neighboring peptides

were from Innovagen. The radiolabeled peptide-binding assay was performed as described [26].

Flow Cytometry and Transmission Electron Microscopy

For flow cytometry, stationary phase bacteria (10^9 colony forming units/ml) were washed and resuspended in phosphate buffered saline (PBS) containing 1% bovine serum albumin (BSA) followed by addition of Ln (Engelbreth-Holm-Swarm murine sarcoma basement membrane, Sigma-Aldrich). The samples were incubated at 37° C for 1.5 h. Bacteria were thereafter washed in PBS + 1% BSA, and incubated with rabbit anti-Ln pAb (Sigma-Aldrich). After washing, fluorescein isothiocyanate (FITC)-conjugated swine anti-rabbit pAb (Dako) were added. Finally, bacteria were analyzed by flow cytometry (EPICS XL-MCL, Beckman Coulter). Ten thousand events were measured for each sample. Transmission electron microscopy (TEM) was performed as described previously [17].

Bacterial Adherence Assays

Adherence of NTHi to immobilized Ln was studied by bacterial probing over Ln-coated glass slides [17]. NTHi adherence to mammalian cell lines and primary cells was analyzed using [^{3}H]-thymidine pulsed bacteria as described [19]. Blocking was conducted with 20 µg antibodies per well.

Enzyme-linked Immunosorbent Assay (ELISA)

Laminin binding to rPF fragments were studied with an indirect ELISA as described [17]. Recombinant truncated PF fragments (50 nM) and synthetic PF peptides (1 µM) were immobilized on polysorp microtiter plates (Nunc). Blocking was done with PBS containing 5% milk for 1 h at RT. For the binding-inhibition assay, Ln (10 nM) was pre-incubated with PF peptides (0-5 µM) at 37 °C for 1.5 h. The suspension was thereafter transferred to plates coated with rPF^{12-293} and the binding was measured as described above. In the direct cell ELISA, cells were grown to confluency in 96-well plates (Nunc) and fixed with 2% formaldehyde 30 min at RT. Thereafter, cells were incubated with PF and subsequently rabbit anti-PF pAb. Horseradish peroxidase-conjugated anti-rabbit pAb (Dako) was used as the secondary layer for all ELISA.

Statistical Analyses

We used Student's *t*-test and Mann-Whitney *U*-test for statistical analyses of two parametrical sets of data and two non-parametrical sets of data, respectively. Two-way ANOVA was employed for statistical analyses of several sets of data. Statistical analyses were performed using GraphPad Prism 5 (GraphPad Software). $P \leq .05$ was considered statistically significant (*, $P \leq .05$; **, $P \leq .01$; ***, $P \leq .001$).

RESULTS

Protein F Is Surface-Associated and Has a Tertiary Structure Similar to the Streptococcal Laminin-Binding Proteins

We have recently identified Protein F (PF), an NTHi protein involved in serum-resistance (Su *et al.*, submitted). The *hpf* gene encodes an uncharacterized 30 kDa iron-chelating protein and is one of four structural genes in an ABC-transporter operon. The operon is present in all available NTHi genomes in the Genbank (n=20) and is highly conserved (>98% identity) (data not shown). To experimentally examine the subcellular localization of PF and determine whether it is exposed on the bacterial surface, we constructed an isogenic NTHi 3655 Δ*hpf* mutant (supplementary Figure S1A). The physiological fitness of the mutant did not differ from the parental strain regarding the whole cell protein profile but a slightly slower growth was observed in soluble medium (data not shown). Transcription analysis showed that the other genes in the operon remained actively expressed in the isogenic mutant (data not shown). Using TEM, gold-labeled anti-PF pAb was shown to recognize PF at the surface of NTHi 3655, but not the PF-deficient mutant (Figure 1A). Since the affinity purified anti-PF pAb were highly specific for PF (supplementary Figure S1B), this experiment suggested that PF is a surface exposed protein.

To elucidate the characteristics of the protein, we analysed the tertiary structure of PF by using homology modeling. The manganese-binding protein MntC of cyanobacteria *Synechocystis* spp. (PDB database code; 1XVL) was found to be the closest structure-solved homolog with 343 bits alignment score (52.1% identity/ 67.0% similarity) and was therefore used as the modeling-template. The superimposition of PF with MntC is shown in Figure 1B. The structural model revealed that PF is constituted by distinct

N- and C-terminal globular domains that are interlinked by a long helix backbone. A metal-binding active site is present between both lobes (shown in sticks). Since the Ln-binding proteins Lbp of *S. pyogenes* (PDB code; 3GI1) and Lmb of *S. agalactiae* (PDB code; 3HJT) belong to the same bacterial ABC-transporter family, we superimposed PF with their crystal structures. Interestingly, despite the weak primary sequence similarity (Lbp 28.3% identity/ 46.9% similarity, and Lmb 28.0% identity/ 46.3% similarity), we observed a strong resemblance in the secondary structure and folding of PF (grey) and Lbp/Lmb (blue/yellow) (Figure 1C) [21].

Protein F Is a Ubiquitous Laminin-Binding Protein of *Haemophilus influenzae*

The structural resemblance between PF and Lbp/Lmb prompted us to investigate the potential Ln-binding capacity of PF. To study the PF-Ln interaction at the bacterial surface, we incubated NTHi 3655 wt and the PF-deficient NTHi 3655 Δ*hpf* with increasing concentrations of soluble Ln. The unbound Ln-fraction was thereafter washed away and bacterial Ln-binding analyzed by flow cytometry. Our data showed that the isogenic Δ*hpf* mutant bound significantly less Ln compared to the NTHi 3655 wt ($p \leq 0.05$) (Figure 2A and 2C).

To prove the Ln-binding property of PF at the bacterial surface, we introduced the *hpf* open reading frame into a heterologous *E. coli* host. After induction of *hpf* expression, we observed a Ln-binding phenotype in the PF-producing *E. coli* when compared to the control *E. coli* containing the empty plasmid (Figure 2B-C). Further analysis of the Ln-interaction at the bacterial surface was conducted using TEM. The isogenic NTHi 3655 Δ*hpf* showed a marked reduction in Ln-binding compared to the parental strain (Figure 2D). Moreover, co-localization of gold-labeled Ln (10 nm) and PF

(detected by gold-labeled anti-PF pAb; 5 nm) was observed at the surface of both PF-producing NTHi 3655 and *E. coli* (Figure 2E).

To study the functional bacterial binding to immobilized Ln, which is more representative of the in vivo basement membrane, Ln was coated on glass slides and incubated with various samples of NTHi and *E. coli* adjusted to the same cell density (OD_{600} = 1.0). NTHi 3655 Δ*hpf* displayed a markedly weaker adherence to immobilized Ln compared to the NTHi 3655 wt (Figure 2F). In parallel, PF-producing *E. coli* adhered to the Ln-coated glass slides, whereas the control *E. coli* did not. Taken together, the co-localization of PF and Ln at the surface of NTHi 3655 in addition to the PF-dependent Ln-binding of heterologous host *E. coli*, suggest that PF is directly involved in Ln-binding at the bacterial surface.

We further wanted to evaluate the Ln-interacting role of PF in a series of clinical NTHi isolates from patients with upper respiratory tract infection. PF-deficient mutants were produced in five clinical isolates and Ln-binding was assessed by flow cytometry (Figure 3A). A consistent decrease in Ln-binding was observed in all strains in the absence of PF. The results indicate that PF is important for the NTHi-Ln interaction in several clinical isolates.

Protein F Contributes to the Multifactorial NTHi-Dependent Laminin Binding

Currently, there have been two reports regarding Ln-binding proteins in NTHi [17, 18]. To evaluate the relevance of PF in comparison to PE and Hap for the NTHi Ln-interaction, NTHi 3655 wt and knock out mutants were incubated with soluble Ln and binding was measured with flow cytometry (Figure 3B). Our data demonstrated that

all mutants had decreased Ln-binding compared to their wild type counterparts, showing that PE, Hap and PF contribute to the Ln-interaction.

The N-terminal Region Lys23-Glu48 of Protein F Interacts with the C-terminus of the Laminin α-Chain

To study the PF-Ln interaction at the molecular level, a series of recombinant PF (rPF) fragments were produced (Figure 4A, Table S2). The putative Ln-binding region of PF was determined by incubating immobilized truncated rPF fragments with increasing concentrations of Ln. Recombinant PF^{12-293} and rPF^{12-98} bound significantly better when compared to the non-binding fragment rPF^{61-144} ($p \leq 0.001$) (Figure 4B). The N-terminal rPF^{12-98} also exhibited a saturable and dose-dependent Ln binding, whereas no binding was detected to the negative control fragment $rPF^{129-177}$ (Figure 4C).

The Ln-binding region of PF was further analyzed in detail by using 13 synthetic peptides that span the entire PF molecule (Figure 5A). PF^{23-48} was identified as the major Ln-binding region ($p \leq 0.001$) in an indirect ELISA. Moreover, PF^{23-48} exhibited saturable and dose-dependent binding to Ln, whereas the non-Ln binding peptide $PF^{124-148}$ did not (Figure 5B). The specificity of the interaction with Ln was evaluated with a binding inhibition assay in which Ln was pre-incubated with various PF peptides prior to addition to microtiter plates coated with rPF^{12-293} (Figure 5C). The peptide PF^{23-48} inhibited Ln binding to rPF^{12-293}, proving that the PF^{23-48}-Ln interaction was specific. Despite that $PF^{184-209}$ bound Ln (Figure 5A-B), the peptide did not inhibit Ln binding to immobilized rPF^{12-293} (Figure 5C). The N-terminal peptide PF^{23-48} was thus identified as the main Ln-binding region.

To determine the PF-binding domain of the Ln molecule, TEM with Ln and gold-labeled rPF^{12-293} was conducted. As seen in figure 5D, PF consistently bound to the C-terminal part of the cruciform Ln molecule. When the length of the molecule was measured, PF appeared to bind to the C-terminal globular domains (LG1-5) of the Ln α-chain (Figure 5D-E). We conclude that the N-terminal region of PF interacts with the C-terminus of the Ln α-chain as revealed by the peptide mapping approach and TEM.

Protein F Mediates Adhesion of NTHi to Pulmonary Epithelial Cells via a Conserved N-terminal Domain

Since several bacterial Ln-binding proteins, including the aforementioned PE, Hap, Lmb and Lbp, have been reported to interact with epithelial cells [15, 19, 20, 27, 28], we analyzed the cell-adhesive capacity of PF. Epithelial cells were immobilized on a solid surface and incubated with increasing concentrations of rPF^{12-293} (Figure 6A). Recombinant PF bound to both NCI H292 and A549 cell lines in a dose-dependent and saturable manner. To evaluate the influence of PF on bacterial adhesion, NTHi 3655 wt and the PF-deficient Δ*hpf* mutant were pulsed with [^{3}H]-thymidine, incubated with pulmonary epithelial cells and adhesion was measured after washing (Figure 6B). The adherence of NTHi 3655 Δ*hpf* to NCI H292 and A549 was reduced by 32.9% and 64%, respectively, compared to the PF-producing wt. Importantly, the isogenic mutant also showed a significant reduction (36.6%) in binding to primary bronchial epithelial cells obtained from a healthy adult donor ($p \leq 0.05$) (Figure 6B).

To investigate the putative cell-adhesive region of PF, cell lines were probed with iodine-labeled synthetic PF peptides followed by washes and measurement of binding (Figure 6C). Interestingly, the Ln-binding region PF^{23-48} (Figure 5A) also displayed the strongest binding to epithelial cells. Moreover, the bacterial-host cell interaction was significantly reduced ($p \leq 0.05$) when bacteria were pre-incubated with anti-PF^{23-48} pAb, but not with the control anti-PF^{44-68} (Figure 6D). These results thus suggested that NTHi utilizes the same N-terminal PF region for both binding to Ln and attachment to epithelial cells.

Bioinformatic analyses and a detailed database search using BLAST showed that PF orthologs exist in a number of other pathogens. The partial alignment of PF^{23-48} with these is shown in Figure 7A. The orthologs present in several members of the family *Pasteurellaceae*, and other pathogens such as *Eikenella corrodens* and *Yersinia pestis*, have highly similar N-termini (Figure 7A). In addition, *S. pyogenes* and *S. agalactiae* Lbp/Lmp N-terminal sequences display partial similarity to PF^{23-48} (Figure 7B). The 3D model of the cell- and Ln-binding region was analyzed in detail and revealed to comprise two β-sheets and one α-helix, connected by three loops (Figure 7C). Amino acid residues Lys23 and Lys25 in loop-1, Gln34, Asp35, Gln38, Asn39 and Asn43 in the α-helix, as well as Thr46 and Glu48 in β-sheet-2 are exposed on the protein surface as predicted by the model (Figure 7D-E). Thus, the structural analysis shows that the experimentally defined host component-binding region Lys23-Glu48 contains several conserved and charged residues that are accessible for interaction with Ln and host epithelial cells.

DISCUSSION

NTHi has recently been reported to bind to ECM-proteins such as Ln and vitronectin [17, 18, 29]. Here, we report the NTHi ABC-transporter protein PF to be a novel Ln- and cell-binding adhesin. ABC-transporters constitute a large family of proteins that play important roles for bacterial pathogenesis [30]. Although previous reports have suggested similar proteins to be implicated in interactions between Gram-negative bacteria and the host [31-35], this is the first study that shows a Gram-negative ABC-transporter protein directly mediating bacterial adherence to host components.

NTHi primarily colonizes the upper respiratory tract of humans and causes a range of airway infections. A significant rise in the occurrence of invasive NTHi infections has recently been observed, possibly due to a niche opening after the introduction of a capsule polysaccharide-conjugate vaccine against *H. influenzae* serotype b [36, 37]. To disseminate from the primary site of infection, bacteria need to colonize and breach the basement membrane barrier. Pathogen interactions with ECM-proteins are particularly important after epithelial disruption (due to, e.g., chronic inflammation and viral infections), which leaves the basement membrane exposed [5]. This is supported by the fact that NTHi infections are commonly identified in COPD-patients or during co-infections with viral pathogens [3, 38, 39]. Other respiratory tract pathogens, such as *S. pneumoniae, S. pyogenes, Moraxella catarrhalis,* and *Mycobacterium* spp, have also been reported to interact with Ln and thereby augment their virulence [9-16]. Binding to ECM-components such as Ln is thus most likely an important mechanism for bacterial pathogenesis.

In the present study, NTHi Δ*hpf* mutants were shown to lose a significant part of their Ln-binding capacity as compared to the parental PF-producing wt strains. Moreover, expression of *hpf* in the heterologous host *E. coli* verified the role of PF as a Ln-binding protein, and co-localization of PF and Ln could be observed at the surface of PF-producing bacteria. In addition, rPF was shown to bind to both alveolar and bronchial epithelial cell lines and NTHi 3655 Δ*hpf* had a significant reduction in adherence to the cells compared to the parental wt strain. Since NTHi 3655 Δ*hpf* also displayed a significant loss of binding to primary cells, our collective data indicate that PF may be clinically relevant for the course of infection by promoting bacterial adherence to the host epithelium and basement membrane during colonization.

The NTHi adhesins PE (a 16 kDa lipoprotein) and Hap (a 155 kDa autotransporter) have previously been shown to interact with Ln [17, 18]. These proteins share no structural or primary sequence similarity with PF or each other, demonstrating the multifariousness of the NTHi-Ln interaction. We show that PF contributes to NTHi Ln-binding to approximately the same degree as PE and Hap (Figure 3B). Furthermore, our data show that PF interacts with the C-terminus of the Ln α-chain (Figure 5D-E), the same region that PE binds to [17]. As PE and PF are not similar, these data could possibly hint at a general pathogen-specific binding region in the Ln molecule. If there are additional Ln-binding factors in NTHi remains to be elucidated.

Protein F (also annotated as a *Y. pestis yfeA* homologue) has been identified amongst other *H. influenzae* proteins to be upregulated during physiological conditions [40, 41]. Culturing NTHi in sputum obtained from COPD-patients resulted in a 3.9-fold increase in PF concentration. Moreover, during heme- and iron-restricted growth, *H.*

influenzae Rd KW20 was reported to enhance the *hpf*-operon transcription up to 11.8-fold. As the iron-concentration is low in the epithelial mucosa [42], an iron-dependent upregulation of PF may enhance the adhesive capacity of NTHi during the initial colonization of the host. These data suggest that PF is important for NTHi in vivo, possibly mediating adherence and metal ion transport.

The 30 kDa PF shares a strong structural resemblance with streptococcal Ln-binding proteins Lbp and Lmb (Figure 1B), albeit the primary sequence similarities are relatively weak. Preliminary unpublished data from our lab indicate that PF chelates Zn^{2+} in analogy with Lbp/Lmb [21, 22]. Assuming that the proteins share the same Ln-binding mechanism, the interactions could either be mediated by several separate but conserved sites in the tertiary structure, or be confined to a small local region that is highly similar in both proteins. Concurrent Zn^{2+}-binding can be an additional mechanism as has been suggested for *S. pyogenes* Lbp [21], since Ln is also known to bind Zn^{2+} [43]. However, we found that the PF-Ln interaction was unaffected by the divalent cation binding of PF (data not shown), suggesting that the mechanism behind the PF Ln-binding is a protein-protein interaction.

In conclusion, PF is characterized as a novel NTHi adhesin that mediates binding to the basement membrane glycoprotein Ln as well as to human pulmonary epithelial cells. Our data sheds light upon the host colonization strategies of the multifaceted and important respiratory tract pathogen NTHi, and will be the impetus for further studies.

REFERENCES

1. Murphy TF, Faden H, Bakaletz LO, et al. Nontypeable *Haemophilus influenzae* as a pathogen in children. Pediatr Infect Dis J **2009**; 28:43-8.

2. Hallstrom T, Riesbeck K. *Haemophilus influenzae* and the complement system. Trends Microbiol **2010**; 18:258-65.

3. Moghaddam SJ, Ochoa CE, Sethi S, Dickey BF. Nontypeable *Haemophilus influenzae* in chronic obstructive pulmonary disease and lung cancer. Int J Chron Obstruct Pulmon Dis **2011**; 6:113-23.

4. Janson H, Carl n B, Cervin A, et al. Effects on the ciliated epithelium of protein D-producing and -nonproducing nontypeable *Haemophilus influenzae* in nasopharyngeal tissue cultures. J Infect Dis **1999**; 180:737-46.

5. Strieter RM, Mehrad B. New mechanisms of pulmonary fibrosis. Chest **2009**; 136:1364-70.

6. Singh B, Fleury C, Jalalvand F, Riesbeck K. Human pathogens utilize host extracellular matrix proteins laminin and collagen for adhesion and invasion of the host. FEMS Microbiol Rev. **2012**; 36: 1122–1180.

7. Durbeej M. Laminins. Cell Tissue Res **2010**; 339:259-68.

8. Yurchenco PD. Basement membranes: cell scaffoldings and signaling platforms. Cold Spring Harb Perspect Biol **2011**; 3: a004911.

9. Caswell CC, Oliver-Kozup H, Han R, Lukomska E, Lukomski S. Scl1, the multifunctional adhesin of group A *Streptococcus*, selectively binds cellular fibronectin and laminin, and mediates pathogen internalization by human cells. FEMS Microbiol Lett **2010**; 303:61-8.

10. Hytonen J, Haataja S, Gerlach D, Podbielski A, Finne J. The SpeB virulence factor of *Streptococcus pyogenes*, a multifunctional secreted and cell surface molecule

with strepadhesin, laminin-binding and cysteine protease activity. Mol Microbiol **2001**; 39:512-9.

11. Tan TT, Forsgren A, Riesbeck K. The respiratory pathogen *Moraxella catarrhalis* binds to laminin via ubiquitous surface proteins A1 and A2. J Infect Dis **2006**; 194:493-7.

12. Hilleringmann M, Giusti F, Baudner BC, et al. Pneumococcal pili are composed of protofilaments exposing adhesive clusters of Rrg A. PLoS Pathog **2008**; 4:e1000026.

13. Alteri CJ, Xicohtencatl-Cortes J, Hess S, Caballero-Olin G, Giron JA, Friedman RL. *Mycobacterium tuberculosis* produces pili during human infection. Proc Natl Acad Sci U S A **2007**; 104:5145-50.

14. Pethe K, Bifani P, Drobecq H, et al. Mycobacterial heparin-binding hemagglutinin and laminin-binding protein share antigenic methyllysines that confer resistance to proteolysis. Proc Natl Acad Sci U S A **2002**; 99:10759-64.

15. Terao Y, Kawabata S, Kunitomo E, Nakagawa I, Hamada S. Novel laminin-binding protein of *Streptococcus pyogenes*, Lbp, is involved in adhesion to epithelial cells. Infect Immun **2002**; 70:993-7.

16. Ouattara M, Cunha EB, Li X, Huang YS, Dixon D, Eichenbaum Z. Shr of group A *streptococcus* is a new type of composite NEAT protein involved in sequestering haem from methaemoglobin. Mol Microbiol **2010**; 78:739-56.

17. Hallstrom T, Singh B, Resman F, A MB, Morgelin M, Riesbeck K. *Haemophilus influenzae* Protein E Binds to the Extracellular Matrix by Concurrently Interacting With Laminin and Vitronectin. J Infect Dis **2011**; 204:1065-74.

18. Fink DL, Green BA, St Geme JW, 3rd. The *Haemophilus influenzae* Hap autotransporter binds to fibronectin, laminin, and collagen IV. Infect Immun **2002**; 70:4902-7.

19. Ronander E, Brant M, Janson H, Sheldon J, Forsgren A, Riesbeck K. Identification of a novel *Haemophilus influenzae* protein important for adhesion to epithelial cells. Microbes Infect **2008**; 10:87-96.

20. Hendrixson DR, St Geme JW, 3rd. The *Haemophilus influenzae* Hap serine protease promotes adherence and microcolony formation, potentiated by a soluble host protein. Mol Cell **1998**; 2:841-50.

21. Linke C, Caradoc-Davies TT, Young PG, Proft T, Baker EN. The laminin-binding protein Lbp from *Streptococcus pyogenes* is a zinc receptor. J Bacteriol **2009**; 191:5814-23.

22. Ragunathan P, Spellerberg B, Ponnuraj K. Structure of laminin-binding adhesin (Lmb) from *Streptococcus agalactiae*. Acta Crystallogr D Biol Crystallogr **2009**; 65:1262-9.

23. Manolov T, Forsgren A, Riesbeck K. Purification of alpha1-antichymotrypsin from human plasma with recombinant *M. catarrhalis* ubiquitous surface protein A1. J Immunol Methods **2008**; 333:180-5.

24. Poje G, Redfield RJ. Transformation of *Haemophilus influenzae*. Methods Mol Med **2003**; 71:57-70.

25. Singh B, Jalalvand F, Morgelin M, Zipfel P, Blom AM, Riesbeck K. *Haemophilus influenzae* protein E recognizes the C-terminal domain of vitronectin and modulates the membrane attack complex. Mol Microbiol **2011**; 81:80-98.

26. Ronander E, Brant M, Eriksson E, et al. Nontypeable *Haemophilus influenzae* adhesin protein E: characterization and biological activity. J Infect Dis **2009**; 199:522-31.

27. Tenenbaum T, Spellerberg B, Adam R, Vogel M, Kim KS, Schroten H. *Streptococcus agalactiae* invasion of human brain microvascular endothelial cells is promoted by the laminin-binding protein Lmb. Microbes Infect **2007**; 9:714-20.

28. Lafontaine ER, Cope LD, Aebi C, Latimer JL, McCracken GH, Jr., Hansen EJ. The UspA1 protein and a second type of UspA2 protein mediate adherence of *Moraxella catarrhalis* to human epithelial cells in vitro. J Bacteriol **2000**; 182:1364-73.

29. Hallstrom T, Blom AM, Zipfel PF, Riesbeck K. Nontypeable *Haemophilus influenzae* protein E binds vitronectin and is important for serum resistance. J Immunol **2009**; 183:2593-601.

30. Garmory HS, Titball RW. ATP-binding cassette transporters are targets for the development of antibacterial vaccines and therapies. Infect Immun **2004**; 72:6757-63.

31. Gabbianelli R, Scotti R, Ammendola S, Petrarca P, Nicolini L, Battistoni A. Role of ZnuABC and ZinT in *Escherichia coli* O157:H7 zinc acquisition and interaction with epithelial cells. BMC Microbiol **2011**; 11:36.

32. Li MS, Chow NY, Sinha S, et al. A *Neisseria meningitidis* NMB1966 mutant is impaired for invasion of respiratory epithelial cells, survival in human blood and for virulence in vivo. Med Microbiol Immunol **2009**; 198:57-67.

33. Castaneda-Roldan EI, Ouahrani-Bettache S, Saldana Z, et al. Characterization of SP41, a surface protein of *Brucella* associated with adherence and invasion of host epithelial cells. Cell Microbiol **2006**; 8:1877-87.

34. Matthysse AG, Yarnall HA, Young N. Requirement for genes with homology to ABC transport systems for attachment and virulence of *Agrobacterium tumefaciens*. J Bacteriol **1996**; 178:5302-8.

35. Yang M, Johnson A, Murphy TF. Characterization and evaluation of the *Moraxella catarrhalis* oligopeptide permease A as a mucosal vaccine antigen. Infect Immun **2011**; 79:846-57.

36. Resman F, Ristovski M, Ahl J, et al. Invasive disease caused by *Haemophilus influenzae* in Sweden 1997-2009; evidence of increasing incidence and clinical burden of non-type b strains. Clin Microbiol Infect **2010**; 17: 1638-45.

37. Brown VM, Madden S, Kelly L, Jamieson FB, Tsang RS, Ulanova M. Invasive *Haemophilus influenzae* disease caused by non-type b strains in Northwestern Ontario, Canada, 2002-2008. Clin Infect Dis **2009**; 49:1240-3.

38. De Schutter I, De Wachter E, Crokaert F, et al. Microbiology of bronchoalveolar lavage fluid in children with acute nonresponding or recurrent community-acquired pneumonia: identification of nontypeable *Haemophilus influenzae* as a major pathogen. Clin Infect Dis **2011**; 52:1437-44.

39. Murphy TF, Bakaletz LO, Smeesters PR. Microbial interactions in the respiratory tract. Pediatr Infect Dis J **2009**; 28:S121-6.

40. Whitby PW, Vanwagoner TM, Seale TW, Morton DJ, Stull TL. Transcriptional profile of *Haemophilus influenzae*: effects of iron and heme. J Bacteriol **2006**; 188:5640-5.

41. Qu J, Lesse AJ, Brauer AL, Cao J, Gill SR, Murphy TF. Proteomic expression profiling of *Haemophilus influenzae* grown in pooled human sputum from adults with chronic obstructive pulmonary disease reveal antioxidant and stress responses. BMC Microbiol **2010**; 10:162.

42. Ghio AJ. Disruption of iron homeostasis and lung disease. Biochim Biophys Acta **2009**; 1790:731-9.

43. Ancsin JB, Kisilevsky R. Laminin interactions important for basement membrane assembly are promoted by zinc and implicate laminin zinc finger-like sequences. J Biol Chem **1996**; 271:6845-51.

LEGENDS

Figure 1. Subcellular localization of PF and the structural model of the protein. *A,* Gold-labeled anti-PF pAb recognize PF at the NTHi 3655 surface but not at the surface of the isogenic PF-deficient NTHi 3655 Δ*hpf* mutant as revealed by TEM. *B,* Superimposed model of PF (grey) with the template MntC of *Synechocystis* spp. (PDB: 1XVL) shown in green (52.1% identity and 67.0% similarity). *C,* Superimposition of PF (grey) with *S. pyogenes* laminin-binding protein (Lbp) (blue) and *S. agalactiae* laminin-binding protein (Lmb) (yellow). N- and C-terminal domains are indicated with the metal ion-chelating active site residues shown in sticks, situated between both domains. Figures were prepared using PyMOL.

Figure 2. Protein F mediates Ln-binding at the surface of bacteria. *A,* Flow cytometry analysis shows significant differences in the Ln-binding of NTHi 3655 wt and NTHi 3655 Δ*hpf* and *B,* PF-producing *E. coli* acquire previously non-existent Ln-binding as measured by mean fluorescence intensity (mfi)/ bacterium. *E. coli* containing an empty plasmid was used as a control. *C,* Histogram representation of a dataset from *A* and *B*. *D,* Transmission electron microscopy shows a marked decrease of bound Ln (gold-labeled) at the surface of NTHi 3655 Δ*hpf* compared to the parental wt strain. *E,* Arrows point to bound gold-labeled Ln (10 nm) that is co-localized with PF detected by gold-labeled anti-PF pAb (5 nm) at the bacterial surface. The bar indicates 100 nm. *F,* PF promotes NTHi 3655 and *E. coli*-PF adherence to immobilized Ln in a basement membrane-mimicking setting whereas non-PF producing bacteria are seen to exhibit markedly less binding to the Ln-coated surface. The mean of three separate experiments is plotted and error bars indicate the standard error of mean (SEM) (*A*

and *B*). Statistical analysis was performed using two-way ANOVA and $P \leq 0.05$ was considered statistically significant (*, $P \leq 0.05$; **, $P \leq 0.01$; ***, $P \leq 0.001$).

Figure 3. Protein F mediates Ln-binding in clinical isolates and contributes to the NTHi-dependant Ln-binding in analogy with PE and Hap. *A*, Flow cytometry analysis show that five clinical isolates display markedly decreased Ln-binding capacity when PF is knocked out, as compared to the PF-producing parental wild type strains. *B*, Comparison of PF, PE and Hap-deficient mutants shows that the absence of all three proteins causes a decline in Ln-binding (used Ln concentration 2.5 nM). The mean of three separate experiments is plotted in both graphs, error bars indicate the standard error of mean (SEM) and statistical differences are between wild type and mutants. Statistical analysis was performed using two-way ANOVA and $P \leq 0.05$ was considered statistically significant (*, $P \leq 0.05$; **, $P \leq 0.01$; ***, $P \leq 0.001$).

Figure 4. Recombinant PF binds Ln via a region in PF $^{12\text{-}98}$. *A*, Coomassie-stained SDS-PAGE gel showing the purified recombinant truncated PF-fragments. *B-C*, rPF$^{12\text{-}98}$ contains the Ln-binding region and binds to Ln in a dose-dependent and saturable manner. Statistical analysis was performed using Mann-Whitney *U*-test. The mean of three separate experiments is plotted in *B*. In *C*, one set of data of three similar experiments is shown. Error bars indicate the standard error of mean (SEM) in all experiments.

Figure 5. PF$^{23\text{-}48}$ interacts with the C-terminus of the cruciform Ln macromolecule α-chain. *A*, To more precisely define the Ln-binding region of PF, a series of synthetic peptides spanning the entire PF molecule were produced. Two potential Ln-binding

regions were identified using an indirect ELISA; PF^{23-48} (consistent with the data from the recombinant fragments) and $PF^{184-209}$. *B,* Ln binds to PF^{23-48}, and to a lesser degree $PF^{184-209}$, in a dose-dependent and saturable manner. C, Only PF^{23-48} binds specifically to Ln and inhibits the interaction with rPF^{12-293}. *D,* Electron microscopy show gold-labeled rPF^{12-293} binding to the Ln α-chain C-terminus (as indicated by white arrows). *E,* Schematic representation of the Ln hetereotrimer showing the α-, β- and γ-chains that form the cruciform molecule. The PF-binding α-chain C-terminal globular domains are indicated by an arrow. Statistical analysis was performed using Mann-Whitney *U*-test and error bars indicate the SEM for all experiments. The mean of three separate experiments are shown in *A* and *C*, whereas three separate experiments were performed with the same outcome for *B*, of which one set of data is shown. $P \leq 0.05$ was considered statistically significant (*, $P \leq 0.05$; **, $P \leq 0.01$; ***, $P \leq 0.001$).

Figure 6. PF promotes NTHi adherence to pulmonary epithelial cells via the N-terminus. *A,* A direct ELISA shows that PF binds to fixed and immobilized NCI H292 and A549 in a saturable and dose-dependent manner. *B,* Deletion of *hpf* results in a marked decrease in the adhesion of NTHi to pulmonary epithelial cell lines as well as to primary bronchial epithelial cells from a healthy adult donor. *C,* PF^{23-48} shows the strongest binding to both cell lines as revealed by a radiolabeled peptide adherence assay. *D,* The NTHi interaction with A549 cells can be inhibited by epitope specific anti-PF^{23-48} pAb but not with anti-PF^{44-68}. The mean of three separate experiments is used for all panels and error bars indicate the SEM in all experiments. Student's *t*-test was used for statistical analyses in panel *B* and two-way ANOVA in panel *D*. $P \leq 0.05$ was considered statistically significant (*, $P \leq 0.05$; **, $P \leq 0.01$; ***, $P \leq 0.001$).

Figure 7: Bioinformatic analyses of PF^{23-48}. *A,* PF homologs are present in other pathogens of the *Pasteurellaceae* family including *H. parainfluenzae, H. somnus, H. parasuis, H. ducreyi, Pasteurella dagmatis, P. multocida, Aggregatibacter aphrophilus, A. segnis, Actinobacillus actinomycetemcomitans,* as well as *Yersinia pestis* and *Eikenella corrodens* belonging to other families. Partial alignment shows the highly conserved nature of the Ln-binding region. *B,* Alignment of PF^{23-48} with Lbp and Lmb of *S. pyogenes* and *S. agalactiae,* respectively. *C,* A cartoon of PF^{23-48} with numbered β-sheets, α-helix and loops with their side chains shown as a ball-and-stick model. *D,* The surface of the PF molecule. The Ln-binding region (encircled) is shown with colors indicating the charge distribution (blue represents positively charged and red negatively charged residues at the surface). *E,* The PF^{23-48} surface (encircled in *C*) is zoomed in. Figures were prepared using PyMOL.

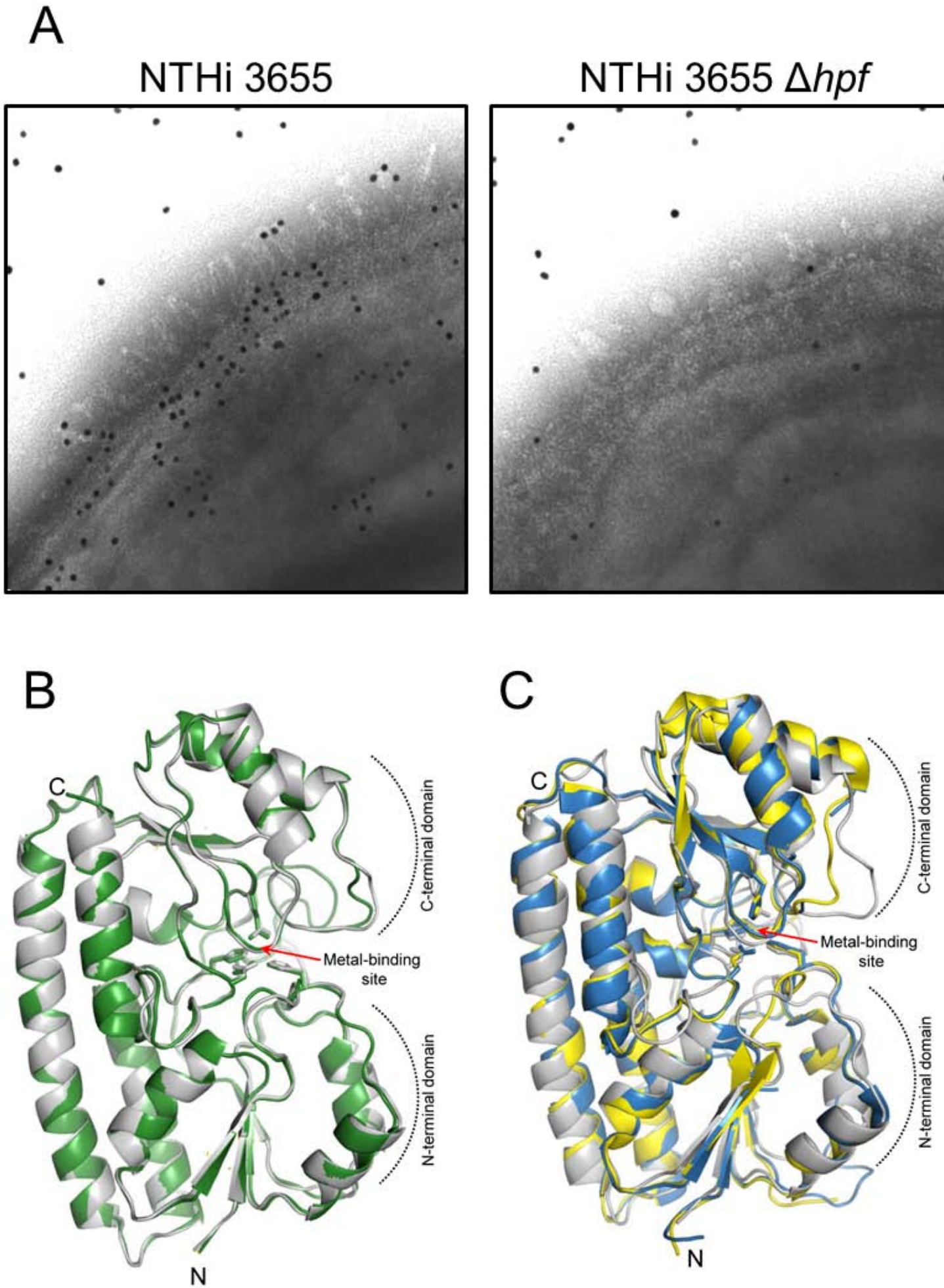
A
NTHi 3655
NTHi 3655 Δhpf
B
C
C
N
C-terminal domain
N-terminal domain
Metal-binding site
C
N
C-terminal domain
N-terminal domain
Metal-binding site

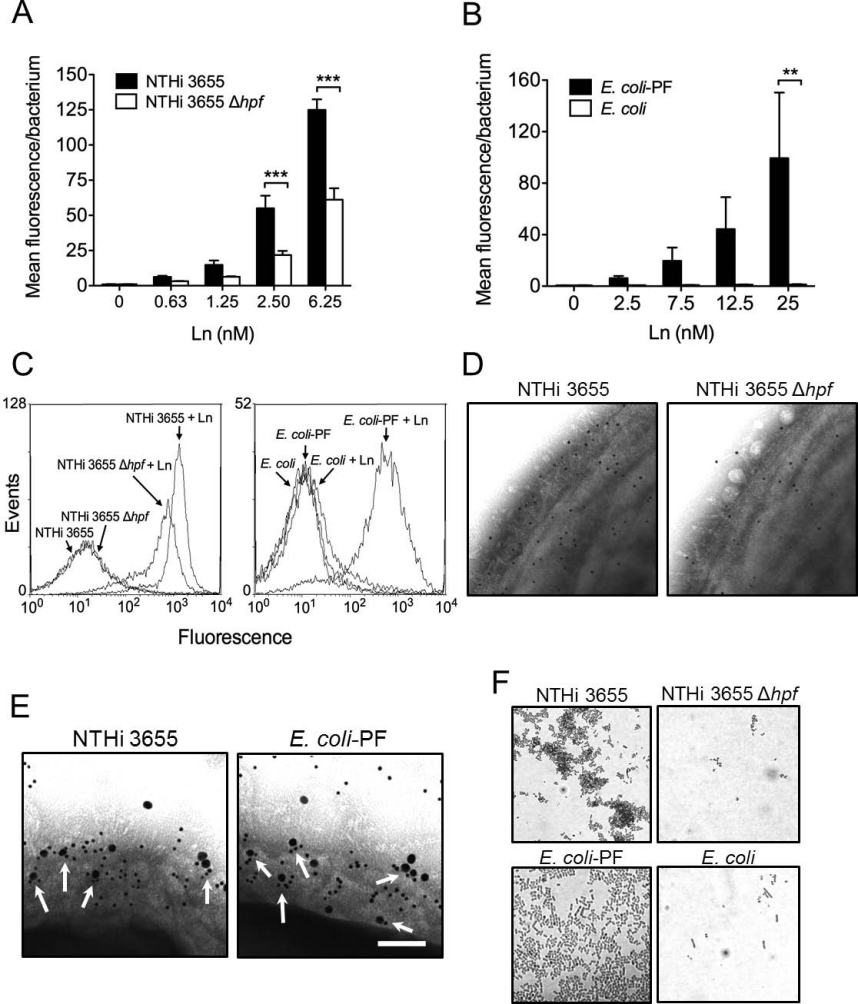
A
Mean fluorescence/bacterium
NTHi 3655
NTHi 3655 Δhpf
***
***
Ln (nM)
B
Mean fluorescence/bacterium
E. coli-PF
E. coli
**
Ln (nM)
C
Events
NTHi 3655 + Ln
NTHi 3655 Δhpf + Ln
NTHi 3655 Δhpf
NTHi 3655
E. coli-PF
E. coli
E. coli + Ln
E. coli-PF + Ln
Fluorescence
D
NTHi 3655
NTHi 3655 Δhpf
E
NTHi 3655
E. coli-PF
F
NTHi 3655
NTHi 3655 Δhpf
E. coli-PF
E. coli

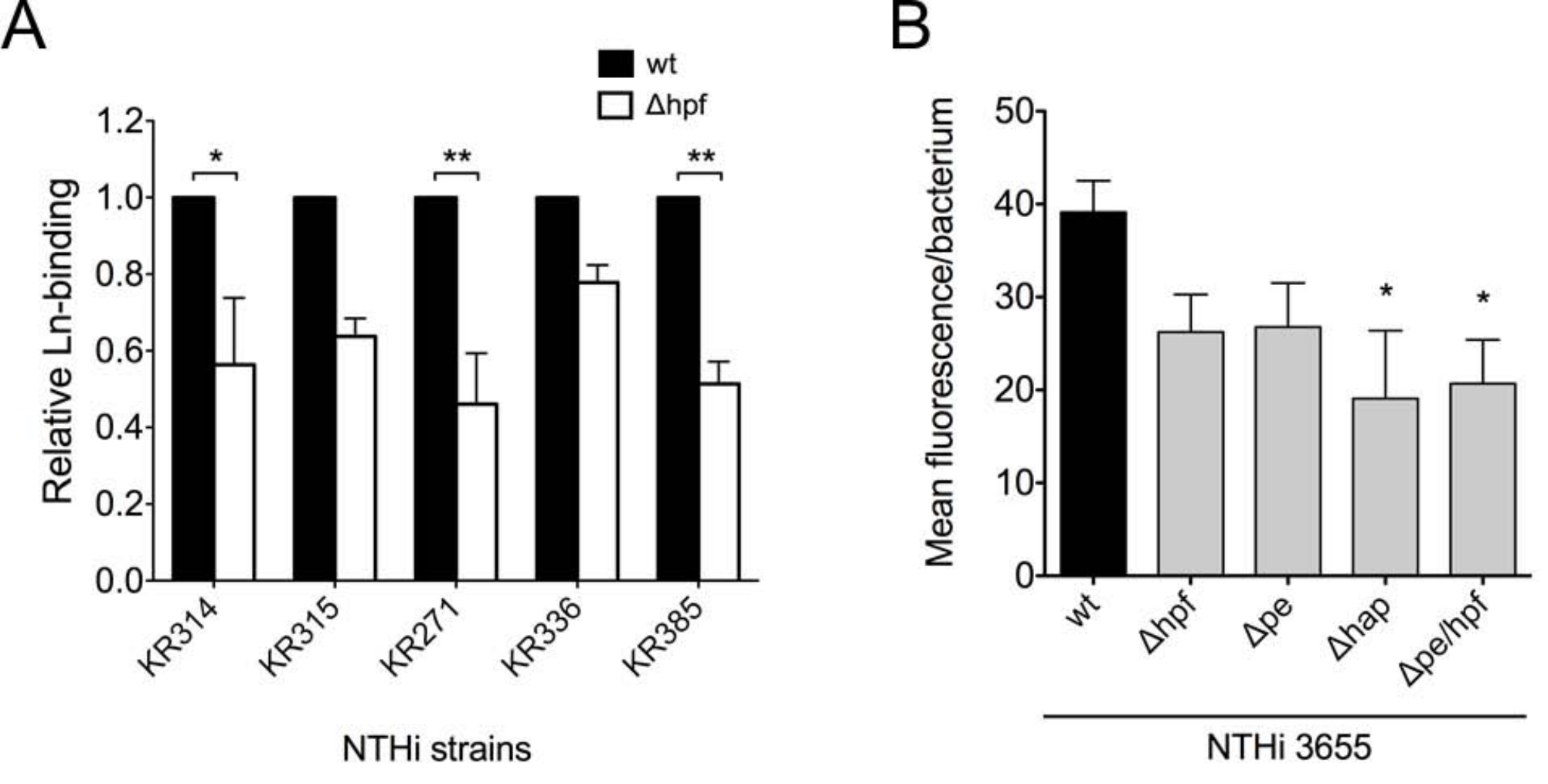
A
wt
Δhpf
Relative Ln-binding
1.2
1.0
0.8
0.6
0.4
0.2
0.0
*
**
**
KR314
KR315
KR271
KR336
KR385
NTHi strains
B
Mean fluorescence/bacterium
50
40
30
20
10
0
*
*
wt
Δhpf
Δpe
Δhap
Δpe/hpf
NTHi 3655

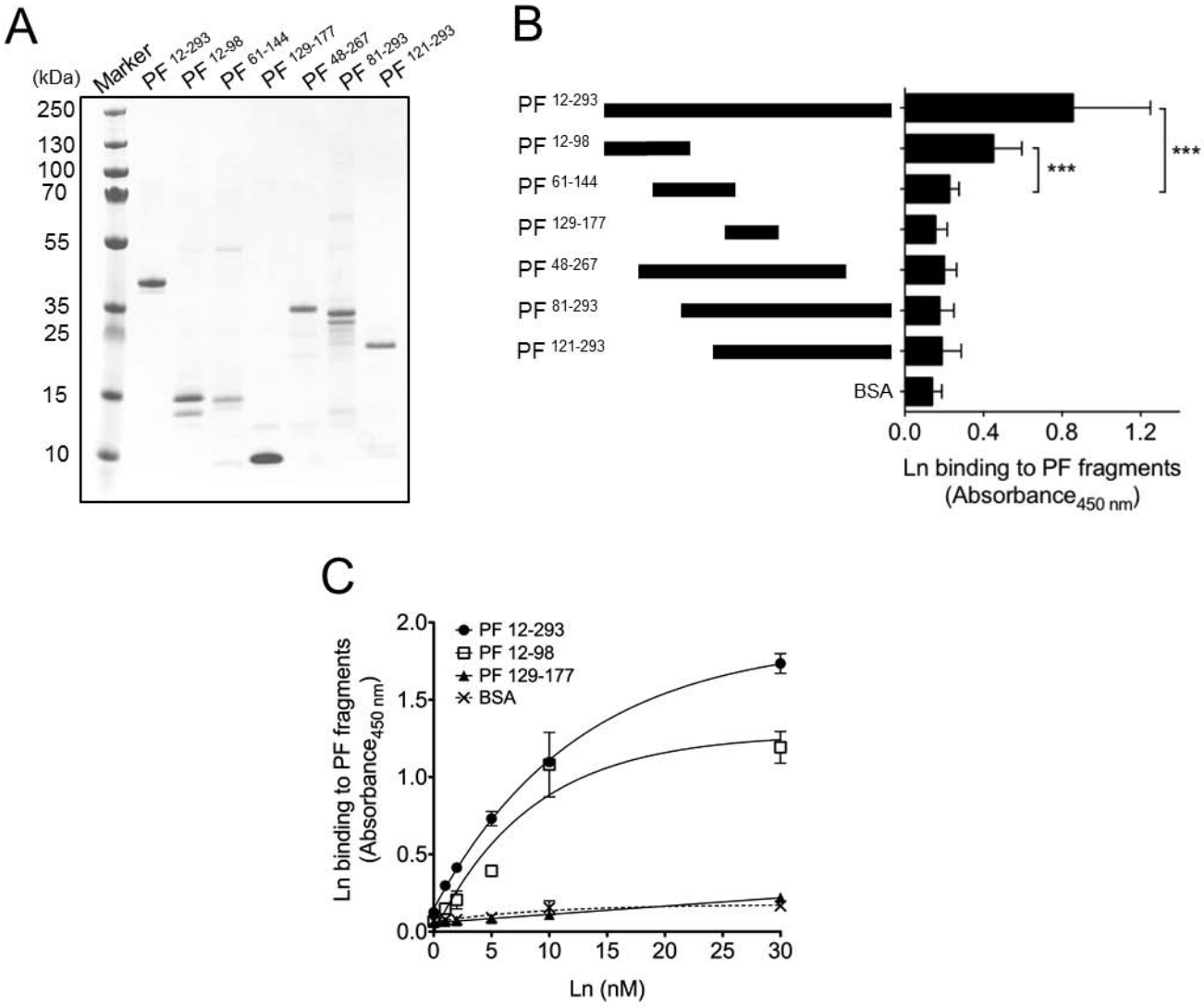
A
(kDa)
Marker
PF 12-293
PF 12-98
PF 61-144
PF 129-177
PF 48-267
PF 81-293
PF 121-293
250
130
100
70
55
35
25
15
10
B
PF 12-293
PF 12-98
PF 61-144
PF 129-177
PF 48-267
PF 81-293
PF 121-293
BSA
***
***
0.0
0.4
0.8
1.2
Ln binding to PF fragments
(Absorbance450 nm)
C
PF 12-293
PF 12-98
PF 129-177
BSA
Ln binding to PF fragments
(Absorbance450 nm)
2.0
1.5
1.0
0.5
0.0
0
5
10
15
20
25
30
Ln (nM)

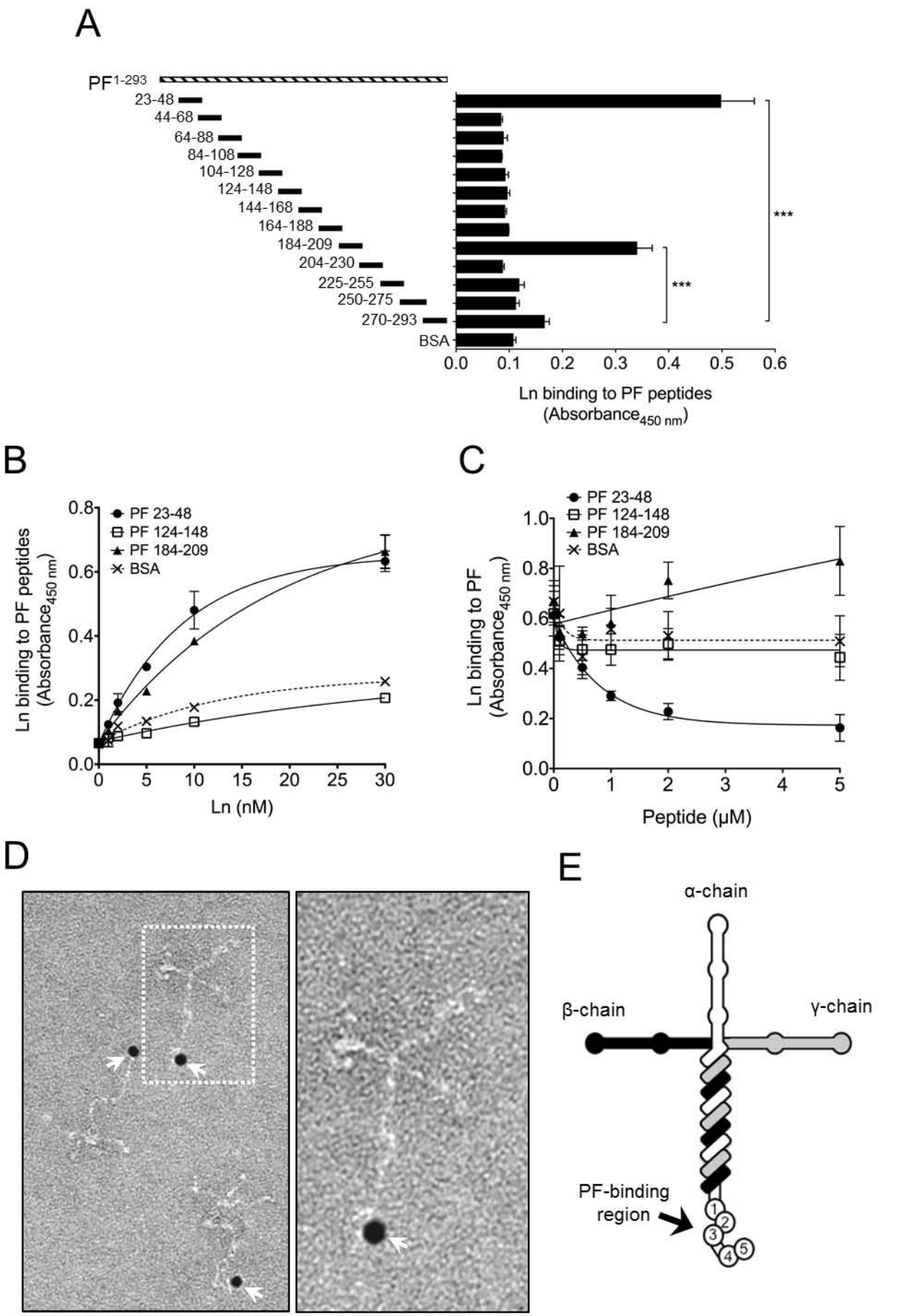
A
PF1-293
23-48
44-68
64-88
84-108
104-128
124-148
144-168
164-188
184-209
204-230
225-255
250-275
270-293
BSA
***
***
0.0
0.1
0.2
0.3
0.4
0.5
0.6
Ln binding to PF peptides
(Absorbance450 nm)
B
PF 23-48
PF 124-148
PF 184-209
BSA
Ln binding to PF peptides
(Absorbance450 nm)
0.0
0.2
0.4
0.6
0.8
0
5
10
15
20
25
30
Ln (nM)
C
PF 23-48
PF 124-148
PF 184-209
BSA
Ln binding to PF
(Absorbance450 nm)
0.0
0.2
0.4
0.6
0.8
1.0
0
1
2
3
4
5
Peptide (μM)
D
E
α-chain
β-chain
γ-chain
PF-binding
region
1
2
3
4
5

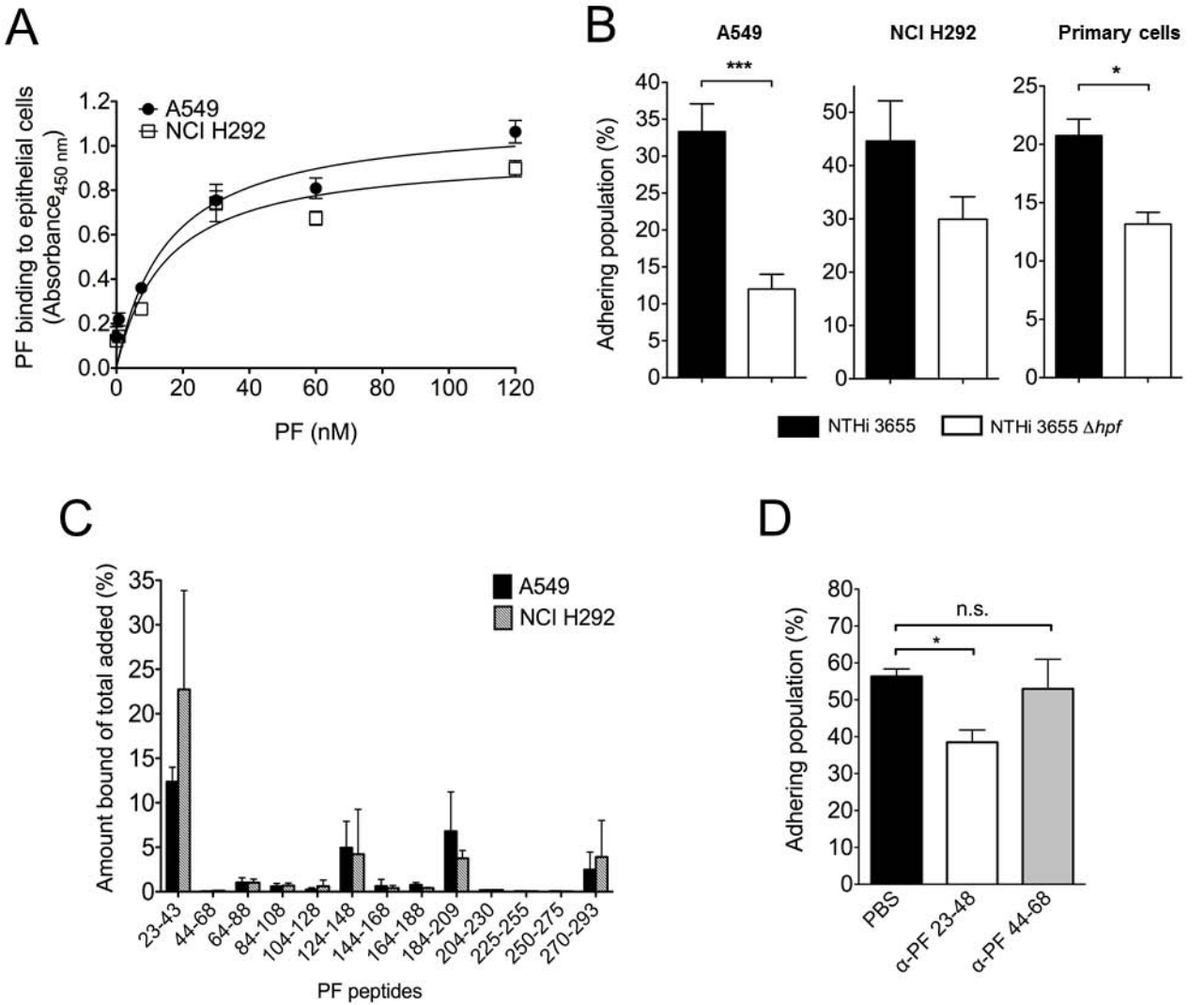
A
PF binding to epithelial cells (Absorbance450 nm)
A549
NCI H292
PF (nM)
B
A549
NCI H292
Primary cells
***
*
Adhering population (%)
NTHi 3655
NTHi 3655 Δhpf
C
Amount bound of total added (%)
A549
NCI H292
23-43
44-68
64-88
84-108
104-128
124-148
144-168
164-188
184-209
204-230
225-255
250-275
270-293
PF peptides
D
Adhering population (%)
n.s.
*
PBS
α-PF 23-48
α-PF 44-68

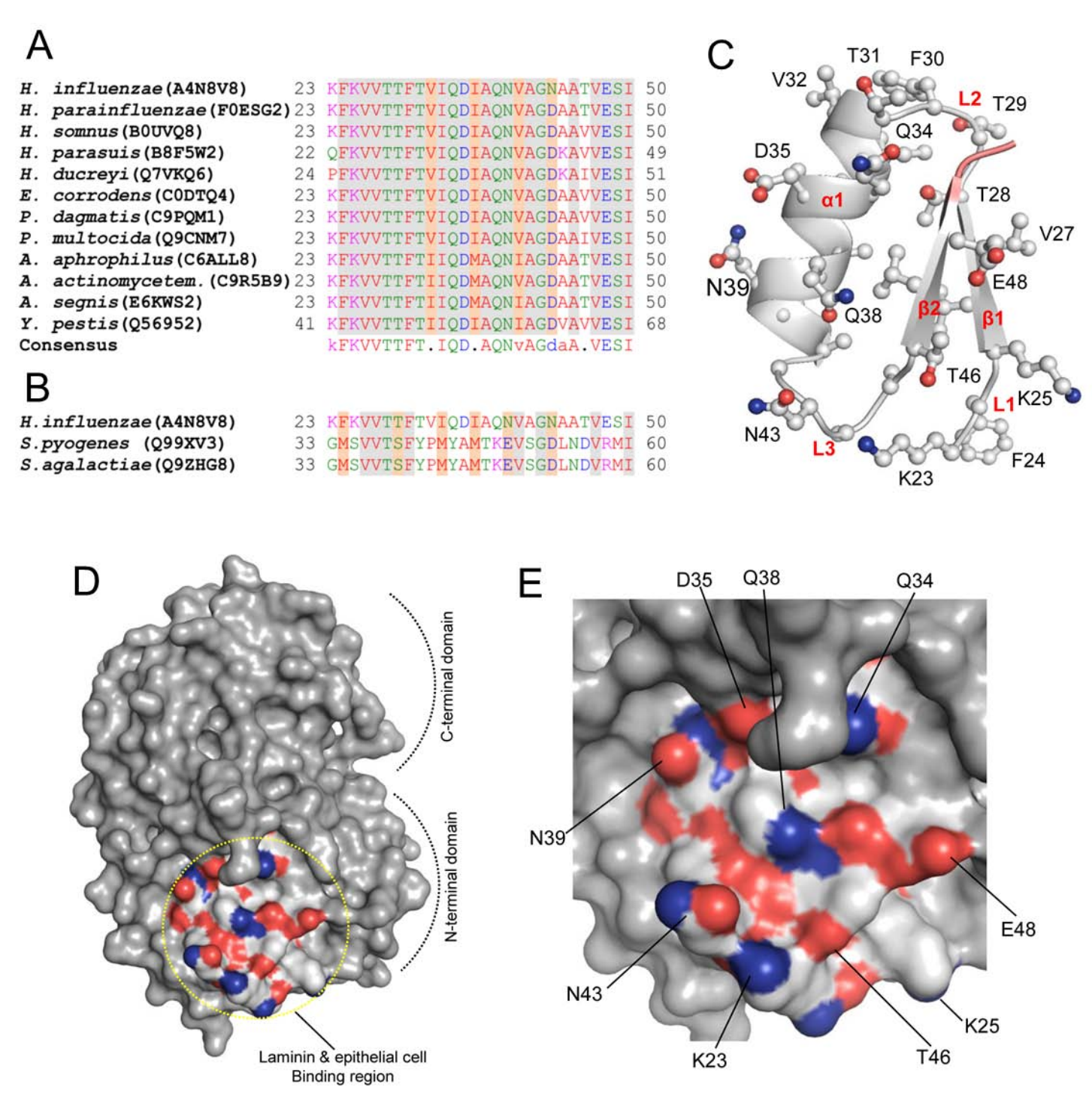
A
H. influenzae (A4N8V8) 23 KFKVVTTFTVIQDIAQNVAGNAATVESI 50
H. parainfluenzae (F0ESG2) 23 KFKVVTTFTVIQDIAQNVAGDAATVESI 50
H. somnus (B0UVQ8) 23 KFKVVTTFTVIQDIAQNVAGDAAVVESI 50
H. parasuis (B8F5W2) 22 QFKVVTTFTVIQDIAQNVAGDKAVVESI 49
H. ducreyi (Q7VKQ6) 24 PFKVVTTFTVIQDIAQNVAGDKAIVESI 51
E. corrodens (C0DTQ4) 23 KFKVVTTFTVIQDIAQNVAGDAAVVESI 50
P. dagmatis (C9PQM1) 23 KFKVVTTFTVIQDIAQNVAGDAAVVESI 50
P. multocida (Q9CNM7) 23 KFKVVTTFTVIQDIAQNVAGDAAIVESI 50
A. aphrophilus (C6ALL8) 23 KFKVVTTFTIIQDMAQNIAGDAATVESI 50
A. actinomycetem. (C9R5B9) 23 KFKVVTTFTIIQDMAQNVAGDAATVESI 50
A. segnis (E6KWS2) 23 KFKVVTTFTIIQDMAQNIAGDAATVESI 50
Y. pestis (Q56952) 41 KFKVVTTFTIIQDIAQNIAGDVAVVESI 68
Consensus kFKVVTTFT.IQD.AQNvAGdaA.VESI
B
H.influenzae (A4N8V8) 23 KFKVVTTFTVIQDIAQNVAGNAATVESI 50
S.pyogenes (Q99XV3) 33 GMSVVTSFYPMYAMTKEVSGDLNDVRMI 60
S.agalactiae (Q9ZHG8) 33 GMSVVTSFYPMYAMTKEVSGDLNDVRMI 60
C
T31
F30
V32
L2
T29
Q34
D35
α1
T28
V27
N39
E48
Q38
β2
β1
T46
L1
K25
N43
L3
F24
K23
D
C-terminal domain
N-terminal domain
Laminin & epithelial cell
Binding region
E
D35
Q38
Q34
N39
E48
N43
K25
K23
T46

Table S1. Primers used for recombinant constructs. Restriction sites are underlined.

Primer name	Sequence 5'-3'	Construct
PF_For12	GCGGATCCGGCACTTGGTTTATTTGCAATGCAAGC	pET26/PF12-293, pET26/PF12-98
PF_For48	CGCGGATCCGGAATCTATTACCAAACCAGGTGC	pET26/PF48-267
PF_For61	CGGGGGATCCGGAACCAACGCCAAAAGAC	pET26/PF61-144
PF_For81	CGCGGATCCGTTAAATTTAGAACGTTGGTTTGAGCG	pET26/PF81-293
PF_For121	GCGGATCCGAATCCACACGCTTGGATGTCG	pET26/PF121-293
PF_For129	CCGGGGATCCGTCTAATGCTTTAATTTATATTGAA	pET26/PF129-177
PF_Rev98	CCCAAGCTTAGGTTTATCTTTAACATT	pET26/PF12-98
PF_Rev144	CCCAAGCTTTTTCACTAACGCATTCT	pET26/PF61-144
PF_Rev179	CCCAAGCTTTTGTGCTAATTTTGCACGAAGCGG	pET26/PF129-177
PF_Rev267	CGCCCAAGCTTAGAAAGTGAATCAACGTACAATACGCCACC	pET26/PF48-267
PF_Rev293	CGCCCAAGCTTTCCGAATCCTTTAACAATAGTTGATAC	pET26/PF12-293, pET26/PF81-293, pET26/PF121-293
PF_KO_ForFR1	ACAGGCTACATTCAAGAATC	Linear *hpf* knock out mutation vector
PF_KO_ForFR2	CAGGGCGGGGCGTAATGGACTCTTTCTCGACATC	Linear *hpf* knock out mutation vector
PF_KO_RevFR1	TCCAGTGATTTTTTTCTCCATAAGATGTCCTTATTTAAAAAAG	Linear *hpf* knock out mutation vector
PF_KO_RevFR2	CCCACTGCGGTACTCAAAAT	Linear *hpf* knock out mutation vector
CmR_For	ATGGAGAAAAAAATCACTGGA	Linear *hpf* knock out mutation vector
CmR_Rev	TTACGCCCCGCCCTG	Linear *hpf* knock out mutation vector
PF_For1_pET16	GCGCCCATGGGAAATTCATTCAAAATTATG	pET16/PF1-293
PF_Rev293_pET16	GCGCCATATGTTTTCCGAATCCTTTAAC	pET16/PF1-293

Table S2. List of recombinant proteins used in the protein-protein interaction studies, with the corresponding information regarding vector background and potential solubilization steps prior to affinity chromatography.

Recombinant fragment	Vector	pelB leader signal sequence	C-terminal His-tag	Harvested from cell fraction	Urea-treatment	Refolded prior to chromatography
PF $^{12-293}$	pET26b	X	X	Cytoplasm		
PF $^{12-98}$	pET26b	X	X	Cytoplasm		
PF $^{61-144}$	pET26b	X	X	Cytoplasm		
PF $^{129-177}$	pET26b	X	X	Cytoplasm		
PF $^{48-267}$	pET26b	X	X	Inclusion body	X	X
PF $^{81-293}$	pET26b	X	X	Inclusion body	X	X
PF $^{121-293}$	pET26b	X	X	Inclusion body	X	X

Figure S1

A

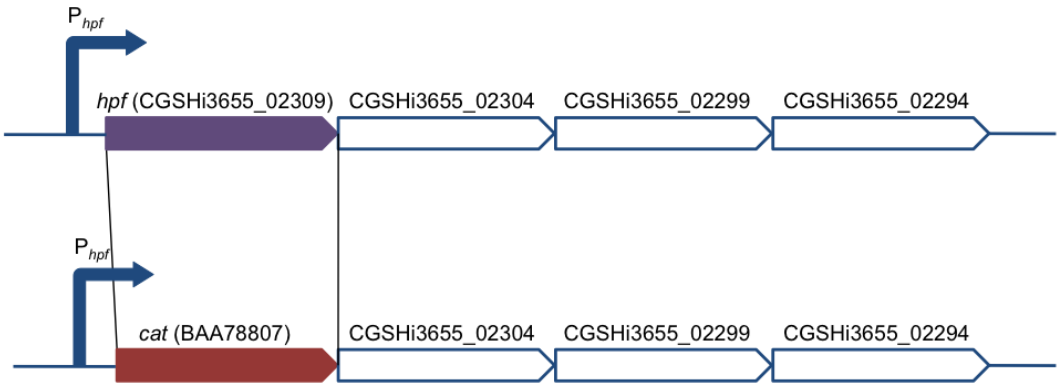

B

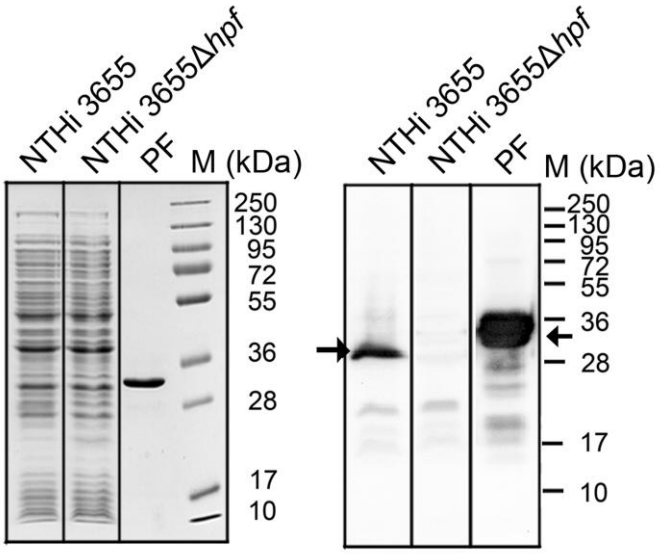

Figure S1. Schematic map of the knock out of *hpf* in NTHi 3655 and proof of the anti-PF polyclonal antibody specificity. *A*, The gene encoding chloramphenicol acetyltransferase (*cat*) was inserted between the upstream and downstream flanking regions of *hpf*, leaving the rest of the operon, as well as the promoter, intact. *B*, Coomassie-stained SDS-PAGE gel (left) and western blot (right) of the total cell lysate of NTHi 3655 wt and Δ*hpf*, showing the specificity of the affinity purified α-PF antibodies (used at a concentration 1:1,500). Recombinant PF (1 ng) was used as a positive control.